Aspect-Ratio Dependence of Charge Transport in Turbulent Electroconvection

Peichun Tsai,[1] Zahir A. Daya,[1,2] and Stephen W. Morris[1]

[1]*Department of Physics, University of Toronto, 60 St. George Street, Toronto, Ontario, Canada M5S 1A7*

[2]*Center for Nonlinear Studies and Condensed Matter & Thermal Physics Group, MS-B258, Los Alamos National Laboratory, Los Alamos, New Mexico 87545, USA*

(Received 19 September 2003; published 26 February 2004)

We present measurements of the normalized charge transport or Nusselt number Nu as a function of the aspect ratio Γ for turbulent convection in an electrically driven film. In analogy with turbulent Rayleigh-Bénard convection, we develop the relevant theoretical framework in which we discuss the local power-law scaling of Nu with a dimensionless electrical forcing parameter $\mathcal{R}$. For these experiments where $10^4 \lesssim \mathcal{R} \lesssim 2 \times 10^5$ we find that $\mathrm{Nu} \sim F(\Gamma)\mathcal{R}^{\gamma}$ with either $\gamma = 0.26$ (± 0.02) or $\gamma = 0.20$ (± 0.03), in excellent agreement with the theoretical predictions of $\gamma = 1/4$ and $1/5$. Our measurements of the aspect-ratio dependence of Nu for $0.3 \leq \Gamma \leq 17$ compares favorably with the function $F(\Gamma)$ from the scaling theory.

DOI: 10.1103/PhysRevLett.92.084503 PACS numbers: 47.27.Te

Heat transport has for many years been the cornerstone in the study of turbulent Rayleigh-Bénard convection (RBC) [1]. Over the past three years there has been remarkable experimental [2–8] and theoretical [9,10] progress in characterizing the properties and mechanisms of heat transfer in fluids heated from below. So far, experiments and theory are relevant only to approximately unit aspect-ratio systems, i.e., geometries that have comparable lateral and vertical dimensions. Turbulent convection flows in nature, however, are laterally extended and the transport of heat across a layer of fluid has been inadequately studied as a function of the aspect-ratio $\Gamma =$ lateral dimension/vertical dimension. In particular, experiments at $\Gamma > 2$ have seldom been performed primarily because it is extremely difficult to achieve the strong forcing that is readily reached in $\Gamma \approx 1$ containers.

In this Letter, we present a study of an electrically driven convecting system which allows a broad range of Γ to be explored at moderate levels of forcing. We find that measurements of the normalized charge transport Nu varies with the aspect-ratio Γ consistent with a function F given by the scaling theory. The strong dependence on Γ, especially for $\Gamma \approx 1$, implies that experiment and theories relevant to this regime are restrictive. The data and the function F become increasingly independent of Γ for $\Gamma \gg 1$. This observation highlights the importance of developing experiments and theory for laterally extended systems where it appears that universal behavior, often lacking in $\Gamma \approx 1$ systems, may be restored [11]. Our data also reveal that $\mathrm{Nu} \sim \mathcal{R}^{\gamma}$ with $\gamma = 0.26$ and 0.20 in agreement with a local power-law scaling theory developed in a manner identical to the Grossmann-Lohse (GL) model for turbulent RBC [9].

In previous work, it has been demonstrated that an electrically conducting, freely suspended liquid crystal film between parallel wires could be driven to convect when a sufficiently large potential drop was applied across its edges [12–18]. Experiments [16,18] and theory [17] were then extended to the naturally periodic geometry of an annular film shown schematically in Fig. 1. Analogous to RBC where an inverted mass density distribution is unstable to buoyant forcing, the thin film has an inverted surface charge density distribution that is unstable to electrical forcing. In this system, an initial bifurcation to convection rolls occurs when the applied voltage V exceeds a critical voltage V_c, corresponding to the critical temperature difference in RBC. At much higher forcing the fluid becomes turbulent but retains the large scale structure of the convection cells.

Electroconvecting smectic films have several advantages and disadvantages relative to traditional RBC experiments. In turbulent RBC experiments, the accurate measurement of heat transport requires detailed accounting of the heat conducted through the sidewalls [3]. The annular geometry of the smectic film [see Fig. 1(a)] is free of lateral boundaries and consequently without sidewall losses, which facilitates precise measurement of the charge transport between the inner and outer electrodes. The film is an annular disk of width $d = r_o - r_i \sim 5$ mm and thickness $s \sim 0.1$ μm. Here r_i (r_o) are the radii of the inner (outer) electrodes that support the film [see Fig. 1(b)]. These radii can be varied so as to achieve different values of Γ. The tiny size of the film, which contains many orders of magnitude less working fluid

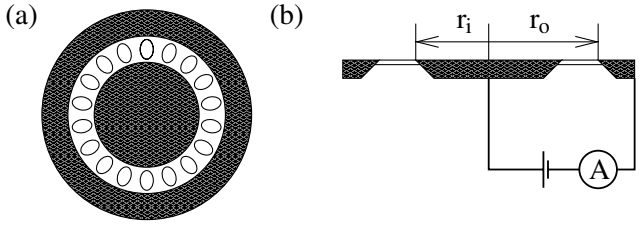

FIG. 1. Schematics of the experiment: (a) top and (b) side.

than required for an RBC experiment, results in data acquisition time scales of minutes, rather than days. On the other hand, the smectic film is delicate and, while many films survive vigorous forcing without thickness change, some do suffer sudden thickness variations. Since V_c and other properties of the flows depend on thickness, these data must be discarded. The dc electrical forcing also results in conductivity drifts in the films, which result in systematic uncertainties. The experiments we describe here were carried out at atmospheric pressure, which increases the film stability. But air drag, which is known to produce a quantitative but not qualitative change to the dissipation, is not properly accounted for in the theory. Nevertheless, notwithstanding these caveats, we are able to efficiently explore the turbulent scaling regime over a wide range of Γ, complementing RBC experiments.

Our experiment consists of a temperature controlled film of octylcyanobiphenyl, a smectic-*A* liquid crystal, suspended between two concentric electrodes. In the smectic-*A* phase, the film flows as an isotropic, incompressible, and Newtonian fluid in the plane of the film. The flow is strictly two dimensional (2D). The film is driven to electroconvect by a dc voltage applied to its inner edge while holding the outer edge at ground potential. The annular assembly is enclosed in a Faraday cage. An experiment consists of imposing a voltage V to the inner electrode and measuring the current I transported through the film with a sensitive electrometer. The applied voltage was varied between 0 and 1000 V in a sequence of small incremental and decremental steps resulting in a current-voltage characteristic. Further details of the apparatus and procedure can be found in Refs. [16–18]. Figure 2 shows a representative current-voltage (IV) characteristic. IV characteristics have been successfully used previously to probe electroconvective turbulence in nematic liquid crystals [19], although the details of the driving mechanism are different in that case. For $V < V_c$ the fluid is quiescent with the current sustained by Ohmic conduction. When $V > V_c$ the fluid is organized in counterrotating vortices, and additional charge is transferred by convection; this is seen by the increase in slope of the IV characteristic. At higher voltages, the fluid becomes turbulent, and the transition is marked by a sudden increase in the rms fluctuations of the current, as shown in the inset of Fig. 2.

A film is a 2D annular sheet. The film has thickness/width $s/d \sim 10^{-4}$. Geometrically, a film is described by its radius ratio $\alpha = r_i/r_o$ and the aspect ratio $\Gamma_r = \pi(r_i + r_o)/(r_o - r_i)$, which is the ratio of the mid-radius circumference to the film width. So defined, $\pi < \Gamma_r < \infty$. To make correspondence with the conventional aspect ratio Γ for RBC, we define $\Gamma = \Gamma_r - \pi$ for the annulus. Two other dimensionless parameters describe the experimental system: $\mathcal{R} = \epsilon_0^2 V^2/\sigma\eta s^2$ and $\mathcal{P} = \epsilon_0\eta/\rho\sigma s d$. Here $\mathcal{R}$ is the control parameter and is a measure of the external electrical forcing and $\mathcal{P}$, the Prandtl-like parameter, is the ratio of the time scales of electrical and viscous dissipation processes in the film. In the above the fluid density, molecular viscosity, and conductivity are denoted by ρ, η, and σ, and ϵ_0 is the permittivity of free space.

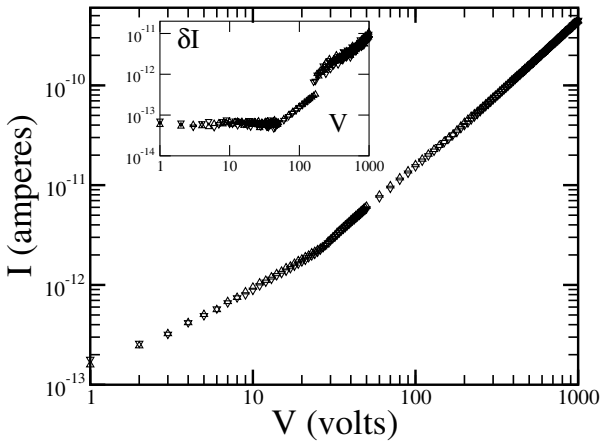

FIG. 2. A representative current-voltage curve for an annular film showing the onset of electroconvection. Data obtained for increasing (decreasing) voltages are shown in $\triangle$ ($\triangledown$). The inset shows the rms fluctuations of the current vs the applied voltage. Here $\Gamma = 6.60 \pm 0.02$ and $\mathcal{P} = 36 \pm 1$.

We normalize the measured total electric current I by the portion due to conduction $I_{\text{cond}} = cV$ where c is the Ohmic conductance of the film obtained from the IV characteristic when the film is not convecting. We define the normalized charge transport or Nusselt number $\text{Nu} = I/I_{\text{cond}}$. Figure 3 shows representative sets of Nu vs $\mathcal{R}$ data at $\Gamma = 0.33 \pm 0.01$ and 6.60 ± 0.02. We find that $\text{Nu} \sim \mathcal{R}^\gamma$ for $10^4 \leq \mathcal{R} \leq 2 \times 10^5$ with either $\gamma = 0.26 \pm 0.02$ or $\gamma = 0.20 \pm 0.03$, depending on the size of $\mathcal{P}$. The error bar is obtained from the variation in the best-fit value of γ over 33 data sets for all five values of Γ.

We developed a theoretical model describing turbulent electroconvection by borrowing from turbulent RBC. The equations of motion that describe electroconvection consist of the incompressible Navier-Stokes equation supplemented with an electrical body force, the charge conservation equation that accounts for Ohmic conduction and advection of charge and Maxwell's equation that relates the surface charge density to the electric potential;

$$\partial_t \mathbf{u} + \mathbf{u} \cdot \nabla \mathbf{u} = -\nabla \frac{p}{\rho} + \nu \nabla^2 \mathbf{u} - \frac{q}{\rho} \nabla \psi, \tag{1}$$

$$\partial_t q + \mathbf{u} \cdot \nabla q = \sigma \nabla^2 \psi, \tag{2}$$

$$q = -2\epsilon_0 \partial_z \psi|_{z=0^+}. \tag{3}$$

These equations are constrained by the no-slip and applied electric potential boundary conditions. In the above equations ∇, $\mathbf{u}$, p, and ν are the 2D gradient, velocity,

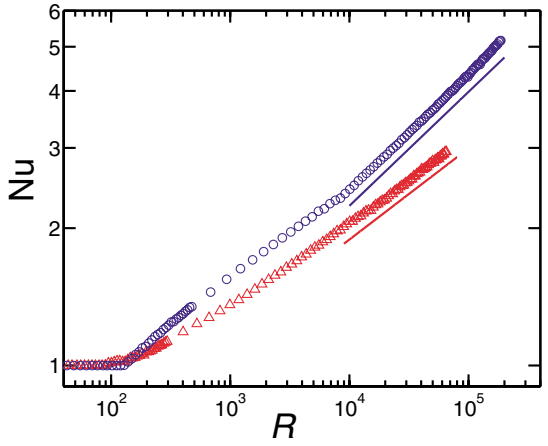

FIG. 3 (color online). Plots of Nu vs $\mathcal{R}$ for $\Gamma = 0.33 \pm 0.01$ ($\triangle$) and 6.60 ± 0.02 ($\bigcirc$). For these $\mathcal{P} = 8.8 \pm 0.3$ and 36 ± 1, respectively. The solid reference lines have slopes of $1/5$ and $1/4$, respectively.

pressure, and kinematic viscosity, respectively. The electric potential ψ is three dimensional and extends outside the film, where $(\nabla^2 + \partial_z^2)\psi = 0$. The Maxwell equation relates the perpendicular gradient of ψ to the surface charge q. The factor of 2 arises from the film's two free surfaces. The relation between ψ and q is thus nonlocal and somewhat complex. It can be considerably simplified by making a local approximation, setting $q = 2\beta\psi$, where β is a certain constant. This local approximation has been shown to be adequate in describing the onset of electroconvection [17].

Equations (1) and (2) are similar to the Boussinesq equations for turbulent RBC. In particular, in the local approximation, there is an almost precise correspondence between the temperature and the electric potential. The periodicity of the annular geometry, and thereby of the velocity and electric potential, allows for exact relations for the globally averaged kinetic and electric dissipations. Denoting averages over the system volume by $\langle \cdots \rangle$ we find the following for the kinetic dissipation $\epsilon_{\mathbf{u}} \equiv \langle \nu(\nabla \mathbf{u})^2 \rangle$ and for the electric dissipation $\epsilon_{\psi} \equiv \langle \sigma(\nabla\psi)^2 \rangle$:

$$\epsilon_{\mathbf{u}} = \frac{\nu^3 \mathcal{R} \mathcal{P}^{-2}(\mathrm{Nu} - 1)}{\ln(1/\alpha)(r_o^2 - r_i^2)(r_o - r_i)^2}, \tag{4}$$

$$\epsilon_{\psi} = \frac{2\sigma V^2 \mathrm{Nu}}{\ln(1/\alpha)(r_o^2 - r_i^2)}. \tag{5}$$

These relations are similar to those for the kinetic and thermal dissipation in RBC presented in Refs. [9,20]. The turbulent flow is composed of unsteady convection cells that tile the annulus as shown in Fig. 1(a). We assume that each cell is roughly square, i.e., it has the same transverse and lateral dimension so that the large scale circulation is then the flow that on average defines a cell. We assume that $\mathrm{Nu} = F(\Gamma) f(\mathcal{R}, \mathcal{P})$, where F and f are unspecified functions. Following the GL theory, we assume that the turbulent flow within each cell can be divided into a laminar boundary layer region and a mixed interior bulk region. We estimate using dimensional arguments the bulk and boundary layer (BL) dissipations: $\epsilon_{\mathbf{u},\psi}^{\mathrm{BULK}}$ and $\epsilon_{\mathbf{u},\psi}^{\mathrm{BL}}$. By balancing these estimates against the exact results in Eqs. (4) and (5), we find that

$$f \sim \mathcal{R}^{\gamma} \mathcal{P}^{\delta}, \qquad \mathrm{Re} \sim \mathcal{R}^{\gamma_*} \mathcal{P}^{\delta_*}, \tag{6}$$

$$F(\Gamma) = \frac{\Gamma + \pi}{\pi} \ln\left(\frac{\Gamma + 2\pi}{\Gamma}\right). \tag{7}$$

As might be expected, we find the same set of exponents γ, δ, γ_*, δ_* that appear in the GL theory. Here, Re is the Reynolds number of the large scale circulation.

In the relatively small $\mathcal{R}$ regime, the dissipation is dominated by the BL contributions $\epsilon_{\mathbf{u}}^{\mathrm{BL}}$ and $\epsilon_{\psi}^{\mathrm{BL}}$. Balancing estimates of these against Eqs. (4) and (5) yield $\gamma = 1/4$ and $\delta = 1/8$. In a neighboring regime where the dissipation is primarily $\epsilon_{\mathbf{u}}^{\mathrm{BULK}}$ and $\epsilon_{\psi}^{\mathrm{BL}}$, the same procedure predicts $\gamma = \delta = 1/5$. Our estimates for the bulk and boundary layer dissipations follow very closely the GL procedure outlined in Section 2.3 of Ref. [9]. Our measured γ exponents, as shown in Fig. 3, are in reasonable agreement with these GL predictions, if we suppose that we traverse the appropriate regimes as $\mathcal{P}$ varies. A detailed validation of the theory depends crucially on either directly demonstrating the correctness of the assumptions about the dominant contributions to the dissipation or on systematically showing that the correct local power-law scalings are, indeed, obtained as one varies $\mathcal{P}$ and $\mathcal{R}$. Our experiments currently span only relatively low $\mathcal{R} < 2 \times 10^5$ and sparsely cover the wide range $5 < \mathcal{P} < 250$. More experiments are needed to adequately test the GL theory for turbulent electroconvection.

In the theoretical treatment described above, we have taken into account the dependence on the aspect ratio of the system, a consideration that was missing in the GL theory which treated only $\Gamma \approx 1$ systems [9,10]. We find that the charge transport is modified by a Γ-dependent factor $F(\Gamma)$. Since the large scale circulation is local to each convection vortex, Re is independent of Γ. Unlike Ref. [20], we find the aspect-ratio dependence is not a power-law scaling but rather a function of the finite annular geometry. We can make a direct comparison with previous turbulent RBC experiments by making a correspondence between the different cell geometries, using $\Gamma = \Gamma_r - \pi$ as described above. We plot $kF(\Gamma)$ vs Γ, with the constant $k = \pi/[(\pi + 1)\ln(2\pi + 1)] = 0.382$. Following Ref. [2], we choose this normalization so that $kF(\Gamma = 1) = 1$. Then $kF \to 0.764$ in the $\Gamma \to \infty$ limit. The function kF decreases monotonically with Γ with the greatest variation for $\Gamma < 2$, and is within 2% of the limiting value for $\Gamma > 7$.

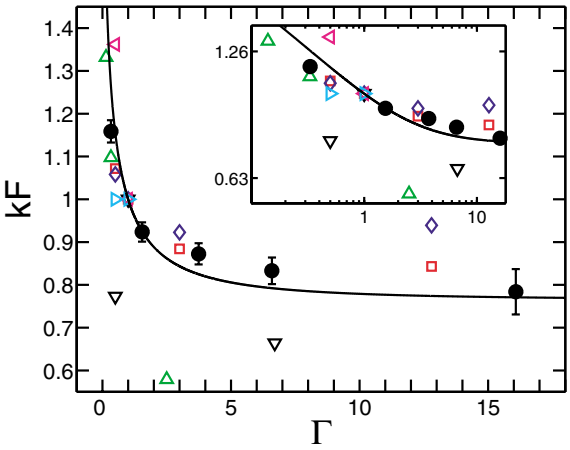

FIG. 4 (color online). The function kF vs Γ. $kF(\Gamma)$ is normalized to unity at $\Gamma = 1$. The solid circles (●) are from the present work. Data from RBC experiments in acetone, with (◇) and without (□) sidewall correction, are from Refs. [2,3]. Also shown are data in air (△), from Ref. [21], helium (▽) from Ref. [22] and (▷) from Refs. [4,8], and water (◁) from Refs. [23]. The inset shows the same data on a logarithmic scale.

Our experimental data span the range $0.3 \leq \Gamma \leq 17$. From power-law fits to Nu vs $\mathcal{R}$ data we have extracted the exponents γ. To determine $F(\Gamma)$ we then divide Nu by $\mathcal{R}^{\gamma}\mathcal{P}^{\delta}$. Because our data extend over a rather wide range of $\mathcal{P}$, we expect to cross regimes with differing γ and δ [9]. To extract the aspect-ratio dependence alone, we used the fitted value of γ, and where $\gamma \approx 0.25$ (0.20), we used the GL-theory prediction of $\delta = 1/8$ (1/5). Using one free parameter for all the data, we again scaled these results so that $F(\Gamma = 1) = 1$. Our data for five different Γ are in reasonable quantitative agreement with the theoretical function F, as shown in Fig. 4. Each data point is an average over 4–10 runs. The error estimates are representative of the scatter in F over these data. In particular, the largest contribution to the error at $\Gamma = 16$ is systematic and arises from the ambiguity in the correct exponent for $\mathcal{P}$.

Data from turbulent RBC experiments [2–4,8,23] for several values of Γ are also broadly in agreement with the function F, in spite of the difference in geometry and the higher range of Rayleigh numbers. Earlier RBC experiments [21,22] used gases as the working fluid and deviate significantly from F.

The strong dependence of F on Γ for $0 \leq \Gamma \lesssim 7$ suggests that the dynamics of turbulent convection is dependent on the system's lateral extent. That the charge or heat transport, a global property, is sensitive to the aspect ratio further suggests that local properties such as temperature and charge fluctuations may be even more strongly dependent on Γ. Experiments in turbulent RBC show that while heat transport is insensitive to cell geometry at fixed $\Gamma \approx 1$, the fluctuations are strongly affected by the shape of the lateral boundary [11]. The relative independence of F on Γ for large aspect ratio $\Gamma \gtrsim 7$ suggests that the normalized charge and heat transport approach a universal value in laterally extended systems. We conjecture that fluctuations in the interior may also become universal in large aspect-ratio systems. Our results emphasize the importance of extending turbulent convection experiments and theories to larger aspect ratios.

We thank G. Ahlers, E. Ben-Naim, R. E. Ecke, and E. Titi for helpful discussions and constructive comments. This research was supported by the Canadian NSERC and the U.S. DOE (W-7405-ENG-36).

[1] L. P. Kadanoff, Phys. Today **54**, No. 8, 34 (2001).
[2] X. Xu, K. M. S. Bajaj, and G. Ahlers, Phys. Rev. Lett. **84**, 4357 (2000).
[3] G. Ahlers, Phys. Rev. E **63**, 015303(R) (2001).
[4] J. J. Niemala, L. Skrbek, K. R. Sreenivasan, and R. J. Donnelly, Nature (London) **404**, 837 (2000).
[5] G. Ahlers and X. Xu, Phys. Rev. Lett. **86**, 3320 (2001).
[6] K.-Q. Xia, S. Lam, and S.-Q. Zhou, Phys. Rev. Lett. **88**, 064501 (2002).
[7] A. Nikolaenko and G. Ahlers, Phys. Rev. Lett. **91**, 084501 (2003).
[8] J. J. Niemela and K. R. Sreenivasan, J. Fluid Mech. **481**, 355 (2003).
[9] S. Grossmann and D. Lohse, J. Fluid Mech. **407**, 27 (2000); Phys. Rev. Lett. **86**, 3316 (2001).
[10] S. Grossmann and D. Lohse, J. Fluid Mech. **486**, 105 (2003).
[11] Z. A. Daya and R. E. Ecke, Phys. Rev. Lett. **87**, 184501 (2001).
[12] S. W. Morris, J. R. de Bruyn, and A. D. May, Phys. Rev. Lett. **65**, 2378 (1990).
[13] S. S. Mao, J. R. de Bruyn, and S. W. Morris, Physica (Amsterdam) **239**, 189A (1997).
[14] Z. A. Daya, S. W. Morris, and J. R. de Bruyn, Phys. Rev. E **55**, 2682 (1997).
[15] V. B. Deyirmenjian, Z. A. Daya, and S. W. Morris, Phys. Rev. E **56**, 1706 (1997).
[16] Z. A. Daya, V. B. Deyirmenjian, S. W. Morris, and J. R. de Bruyn, Phys. Rev. Lett. **80**, 964 (1998).
[17] Z. A. Daya, V. B. Deyirmenjian, and S. W. Morris, Phys. Fluids **11**, 3613 (1999).
[18] Z. A. Daya, V. B. Deyirmenjian, and S. W. Morris, Phys. Rev. E **64**, 036212 (2001); Phys. Rev. E **66**, 015201(R) (2002).
[19] T. Kai, S. Kai, and K. Hirakawa, J. Phys. Soc. Jpn. **43**, 717 (1977); J. T. Gleeson, Phys. Rev. E **63**, 026306 (2001).
[20] B. I. Shraiman and E. D. Siggia, Phys. Rev. A **42**, 3650 (1990); E. D. Siggia, Annu. Rev. Fluid Mech. **26**, 137 (1994).
[21] D. C. Threlfall, Ph.D. thesis, 1974 (unpublished).
[22] X-Z. Wu and A. Libchaber, Phys. Rev. A **45**, 842 (1992).
[23] Y. Shen, P. Tong, and K.-Q. Xia, Phys. Rev. Lett. **76**, 908 (1996).